Supplemental figures "A plug and play microfluidic platform for standardized sensitive low-input Chromatin Immunoprecipitation", Dirks et al., Genome Research 2021

Supplemental Figure 1

Authors: PMID	Year	Technology	Automated ChIP	Microfluidic/ miniaturized	Readout	# of parallel samples	Ease of implementation	Minimum # cells started	Native proteins profiled	Handling time (cells to DNA)	cell readout	Pooled indexed chromatin	Fragmentation
Murphy et al: 29842781	2018	LIFE-ChIP-seq	Yes	Valve microfluidic	NGS	4	Custom PDMS chip, custom operation script	1000000	H3K4me3, H3K27ac	1 day	No	No	Sonication
Cao et al: 26214128	2015	MOW-ChIP-seq	Yes	Valve microfluidic	NGS	1	Custom PDMS chip, custom operation script	10000 to 100	H3K4me3, H3K27ac	Not described	No	No	Sonication
Shen et al: 25178839	2015	-	Yes	Valve microfluidic	NGS	4	Custom PDMS chip, custom operation script	1000	H3K4me3	1 day	No	No	Sonication/MNase
Berguet et al: 25549003	2014	-	Yes	No: Liquid handler robot	NGS	Not specified	Commercial platform (IPStar)	1000000; 10000 (H3K4me3)	H3K4me3, H3K27ac, H3K27me3, H3K9me3	1 day	No	No	Sonication
Gasper et al: 24919486	2014	R-ChIP	Yes	No: Liquid handler robot	NGS	96	Commercial platform (Tecan Freedom EVO 200)	1000000 (Tissue culture dish)	*p300*	Not described	No	No	Sonication
Aldridge et al: 24200198	2013	AHT-ChIP-seq	Yes	No: Liquid handler robot	NGS	96	Commercial platform (Agilent Bravo)	1000000	H3K4me3, CEBPA, RAD21, p300, HNF4A	5 days (400 samples)	No	No	Sonication
Kaya-Okur et al: 31036827	2019	scCUT&Tag	No	No	NGS	n/a	ICELL8 sorting, other operations manual	1	H3K27me3	1 day	Yes	No	Tn5
Ai et al: 31481796	2019	itChIP-seq	No	No	NGS	n/a	FACS, other operations manual	100	H3K4me3, H3K27me3	1.5 days	Yes	Yes	Tn5
Hainer et al: 30955888	2019	uliCUT&RUN	No	No	NGS	n/a	FACS, other operations manual	1	CTCF, SOX2, NANOG,	Not described	Yes	No	MNase
Ku et al: 30923384	2019	scChIC-seq	No	No	NGS	n/a	FACS, other operations manual	1000000	H3K4me3, H3K27me3	2 days	Yes	No	Mnase
Rotem et al: 26458175	2015	Drop-ChIP	No	Droplet microfluidic	NGS	n/a	Requires calibration droplets / merging setup	Not described	H3K4me3, H3K4me2	2 days	Yes	Yes	MNase
Grosselin et al: 31152164	2019	scChIP-Seq	No	Droplet microfluidic	NGS	n/a	Requires calibration droplets / merging setup	15000	H3K4me3, H3K27me3	5 days	Yes	Yes	MNase
van Galen et al: 26687680	2016	Mint-ChIP	No	No	NGS	n/a	All operations manual	5000 to 500	H3K4me3, H327ac, H3K27me3	Not described	No	Yes	MNase
Skene et al: 29651053	2018	CUT&RUN	No	No	NGS	n/a	All operations manual	100 (H3K27me3); 1000 (CTCF)	H3K27me3, CTCF	1 day	No	No	MNase
Dahl et al: 27626377	2016	µChIP-seq	No	No	NGS	n/a	All operations manual	500	H3K4me3, H3K27ac	Not described	No	No	Sonication
Zhang et al: 27626382	2016	STAR ChIP-seq	No	No	NGS	n/a	All operations manual	200	H3K4me3	1.5 days	No	No	MNase
Brind'Amour et al:	2015	ULI-NChIP	No	No	NGS	n/a	All operations manual	1000; 5000 (H3K4me3)	H3K4me3, H3K9me3, H3K27me3	1.5 days	No	No	MNase
Schmidl et al: 26280331	2015	ChIPmentation	No	No	NGS	n/a	All operations manual	10000; 100000 (TFs)	H3K4me3 , H3K4me1, H3K27ac, H3K27me3, H3K36me3, GATA1, PU1	Not described	No	No	Tn5
Wallerman et al: 26195988	2015	lobChIP	No	No	NGS	n/a	All operations manual	1000000	H3K4me3, H3K27ac, H3K27me3, H3K36me3	1 day	No	No	Sonication
Adli & Bernstein: 21959244	2011	nano-ChIP-seq	No	No	NGS	n/a	All operations manual	10000	H3K4me3	4 days	No	No	Sonication
Dahl & Collas: 18202078 & 18536650	2008	µChIP	No	No	qPCR	n/a	All operations manual	1000	H3K4me2 H3K4me3, H3K9me2 H3K9me3 H3K9ac, H3K27me3, RNAPII	1 day	No	No	Sonication
Dahl & Collas: 17272500	2007	Q2ChIP	No	No	qPCR	n/a	All operations manual	100 cells chromatin equivalent	Pou5f1, H3K9ac, H3K9me2, H3K9me3, H3K27me3, H3K4me2, H3K4me3	1 day	No	No	Sonication
O'Neill et al: 16767102	2006	CChIP	No	No	qPCR	n/a	All operations manual	100	H3K4me3, H3K4me1, H3K9me2, H4K16ac	2 days	No	No	MNase

Supplemental Figure 1. Overview of main ChIP-seq procedures pioneered for low-input and/or automated ChIP-seq. In green the features that are advantageous, in red the disadvantageous features, in orange strategies that are compatible with single cell readout. Current automated low-input ChIP-seq workflows require custom-built platforms and can handle only a low number of parallel samples, as also indicated in the red boxes.

Supplemental Figure 2

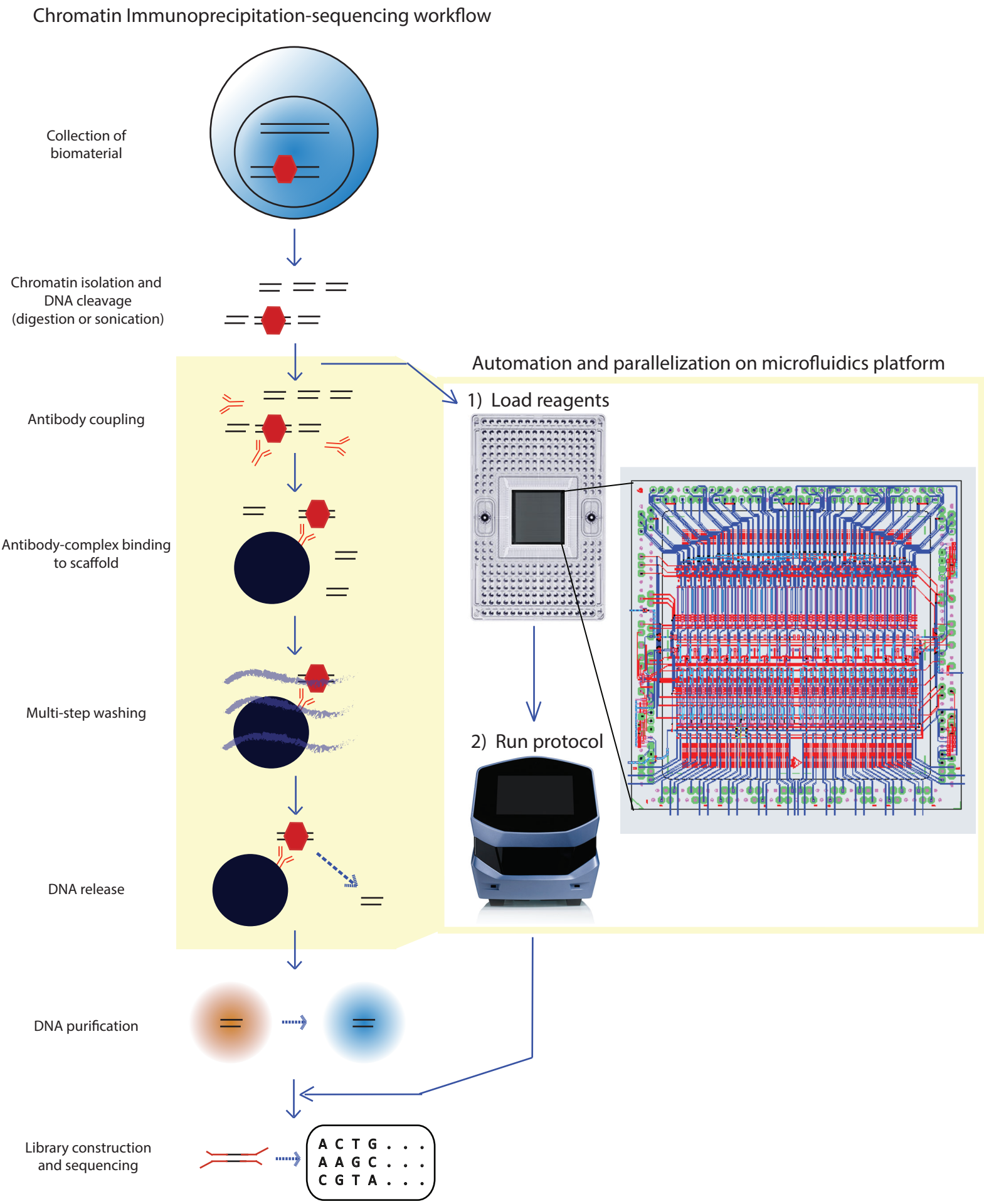

Supplemental Figure 2. Overview of the conventional ChIP-seq workflow and the part of the ChIP-seq workflow that we automated on the microfluidic platform.

Supplemental Figure 3

A

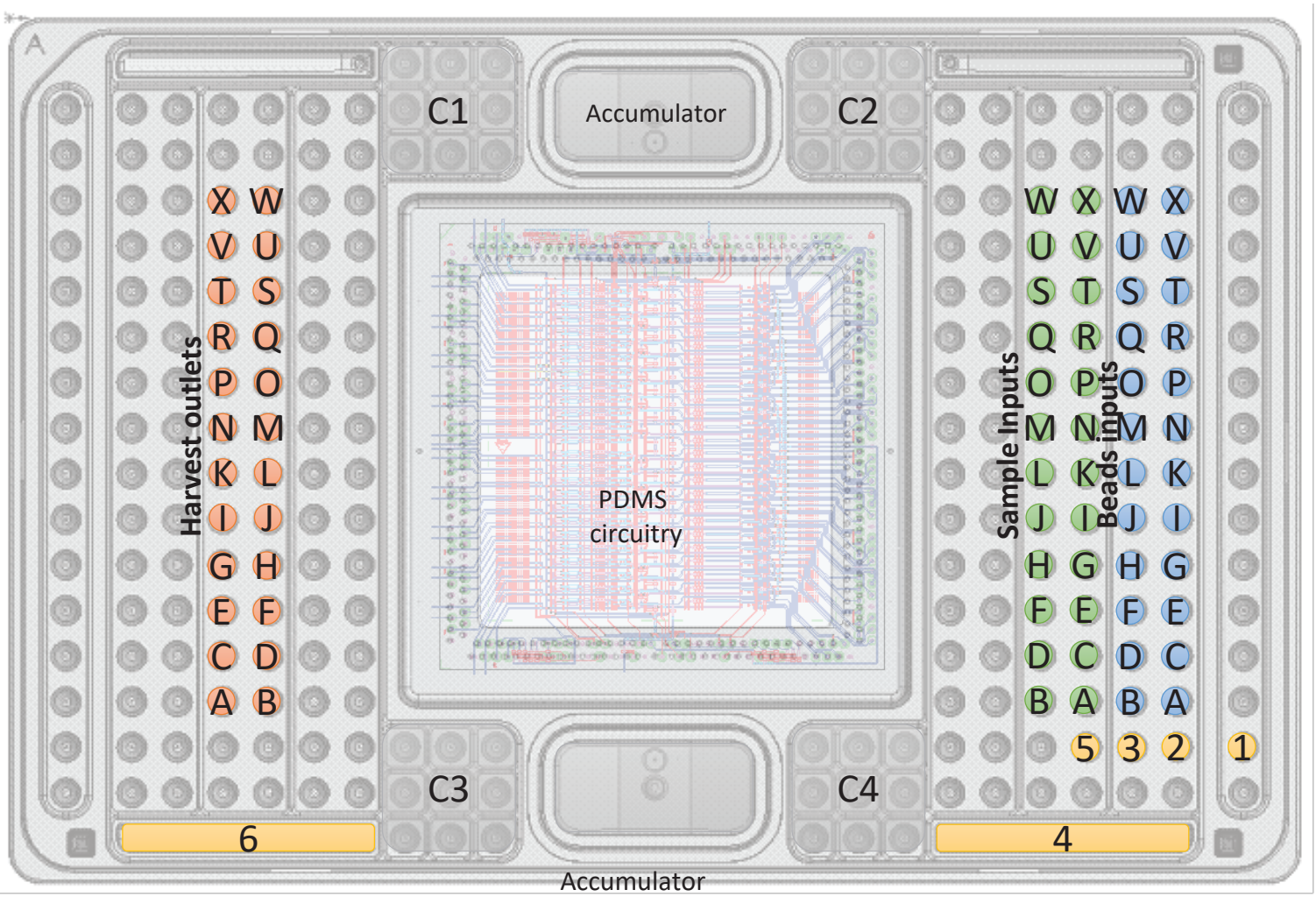

	Carrier inlet	Buffer
	C1, C2, C3, C4	25µL 0.05% Tween-20
	Accumulators	200µL 0.05% Tween-20
	Beads inlet	15µL ProA/G beads
	1	20µL Frit beads
	2	25µL Equilibration buffer
	3	25µL Equilibration buffer
	4	200µL High Salt wash buffer
	5	5µL DNA Extraction buffer
	6	200 µL DNA Elution buffer
	Sample inlet	1-8µL chromatin + antibody
	Harvest outlet	~ 3uL output

B

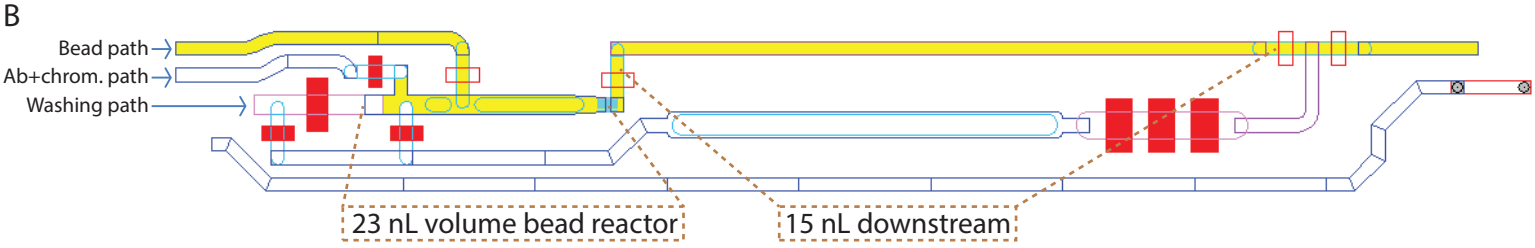

Supplemental Figure 3. Details of the microfluidic IFC. **(A)** Pipette map on the newly developed microfluidic plates for ChIP. All control valves as present in the Integrated Fluidic Circuitries (Fig. 1C) can be individually pressurized by the use of 0.05% Tween 20 solution that is loaded within the wells C1-C4 and within the accumulators. The PDMS circuitry chip is present in the center. **(B)** Volumes of the main parts of a single reactor unit within the microfluidic IFC.

Supplemental Figure 4

A

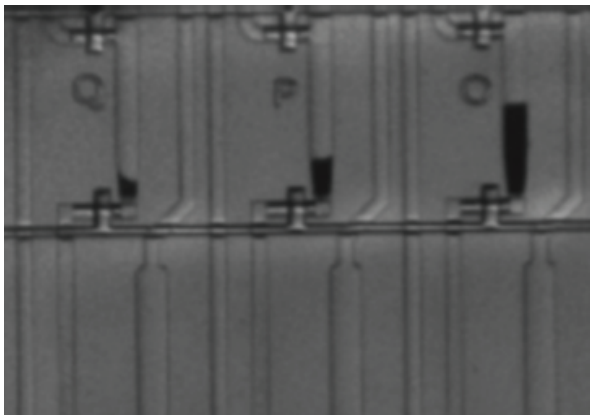

Column size:	Small	Medium	Large
Approximate volume:	1 nL	3 nL	6-9 nL

B

Columns A-F

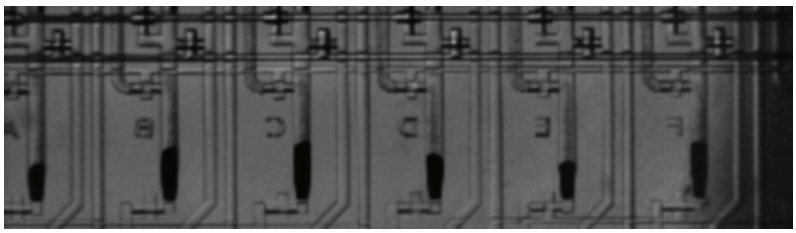

Columns G-L

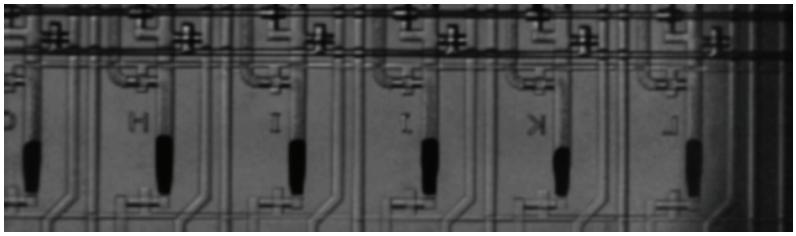

Columns M-R

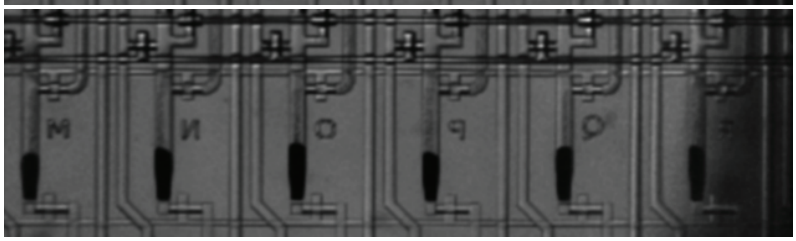

Columns S-X

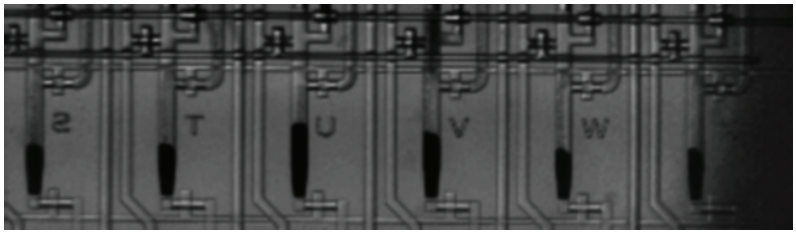

C

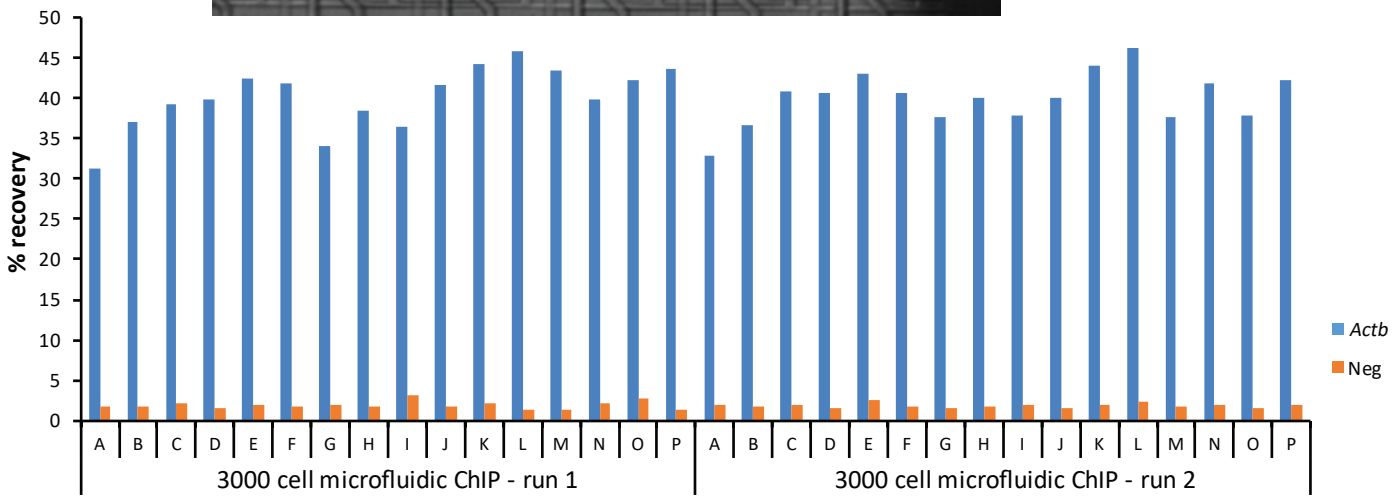

Supplemental Figure 4. Overview and reproducibility of the antibody binding columns as generated within the microfluidic chip for ChIP. **(A)** Phase-contrast image of microfluidic bead columns that are packed to various sizes. **(B)** Reproducibility of bead packing column across the 24 parallel reactors of the Integrated Fluidic Circuit. These are not the exact but representative columns for the experiments as shown in Fig. 2F and Supplemental Fig. S4C. **(C)** Reproducibility of ChIP-qPCR across the 24 parallel reactors of a single microfluidic plate (A-P), and between 2 microfluidic plates run on different days (run 1 and 2), as shown for H3K4me3 per individual ChIP.

Supplemental Figure 5

A

Carrier inlet	Hands-on time
Acquire chromatin, fresh or frozen, crosslinked sonicated or native digested.	--
Combine chromatin with ChIP buffer with antibody of choice	10 minutes
Pre-incubate chromatin at 4°C (30 minutes)	--
Pipette beads, reagents and chromatin into carrier	10 minutes
Run automated ChIP protocol in instrument (4.5 hours)	--
Harvesting	10 minutes
Total	30 minutes

B

Step	Details	Time
1) Load chip	Load microfluidic chip into the controller, pressurize the valves and inlets, priming of valves and reagents to avoid air bubbles in the system.	15 min.
2) Pack column	Primes branch structure and reactors, primes column bypass, packs 5 cycles of ~200 pL frit beads into the reactor, packs ProAG beads into reactor for 10 minutes (~5 nL volume).	30 min.
3) Wash	Removes bead buffer from ChIP column.	10 min.
4) IP	Loads chromatin and antibody across the bead column at the specified pressure for the specified amount of time.	35 min.
5,6) Wash (x2)	Equilibrates the ChIP to physiological salt condition, then performs a high salt wash to remove non-specific binding proteins and DNA segments.	20 min.
7) Air purge	Removes the high salt wash buffer and any remaining non-specific DNA carrying proteins.	10 min.
8) Extraction	Loads a Proteinase K buffer on to the column and increases the temperature to elute specific DNA from the column.	90 min.
9) Harvest	Pushes the specific DNA out of the PDMS circuitry into the carrier for pipetting off-chip.	60 min.

C

Script	Settings, optional tweaks
def info():	
script.requires("LIBRARY");	Load library containing valve operation schematics
script.name="Miniaturized ChIP-seq";	
script.version="X.X";	
def main():	
ChIP_Names()	
NGS_Names()	
AP=30	Anvil pressure
load_chip(True,65,10) (1)	
off('B2')	
ChIPColumn(AP,9,13,5,10) (2)	5x0.05nL frit bead pack at 9 psi, 13 psi ProAG packing for 10 min
AP=35	
DilationWash(AP,EQUILIBRATION,5,4) (3)	Washing cycles, temperature
DirectIP(AP,30,4,11)	Chromatin loading for 30 minutes, 4 °C, 11 psi
set_temp(4)	
DilationWash(AP,AIR PURGE,20,12) (4)	Air purge, 20 cycles of 5nL, 12 psi
DilationWash(AP,EQUILIBRATION,15,12) (5)	150mM NaCl wash, 15 cycles of 5nL, 12 psi
DilationWash(AP,HIGH SALT WASH,15,12) (6)	450mM NaCl wash, 15 cycles of 5nL, 12 psi
DilationWash(AP,AIR PURGE,20,12) (7)	Air purge, 20 cycles of 5nL, 12 psi
set_temp(25)	
AP=40	
Extraction(AP,EXTRACTION,60,65,12,beads='False') (8)	Proteinase K, 60 min. column incubation, 65 °C, 12 psi
AP=30	
set_temp(40)	
HarvestChIP(AP,11,300) (9)	11 psi, 300 harvest cycles of 10nL volume (~3uL)
LockChip(AP)	Output chip

Supplemental Figure 5. Overview of the automated microfluidic protocol that we developed. **(A)** Hands-on and machine time of the newly developed protocol. **(B)** Overview of the running time of the individual steps that are performed during the ChIP on the plates. **(C)** Overview of the adaptable script associated with running of the automated microfluidic for ChIP. Pink numbers refer to panel (B).

Supplemental Figure 6

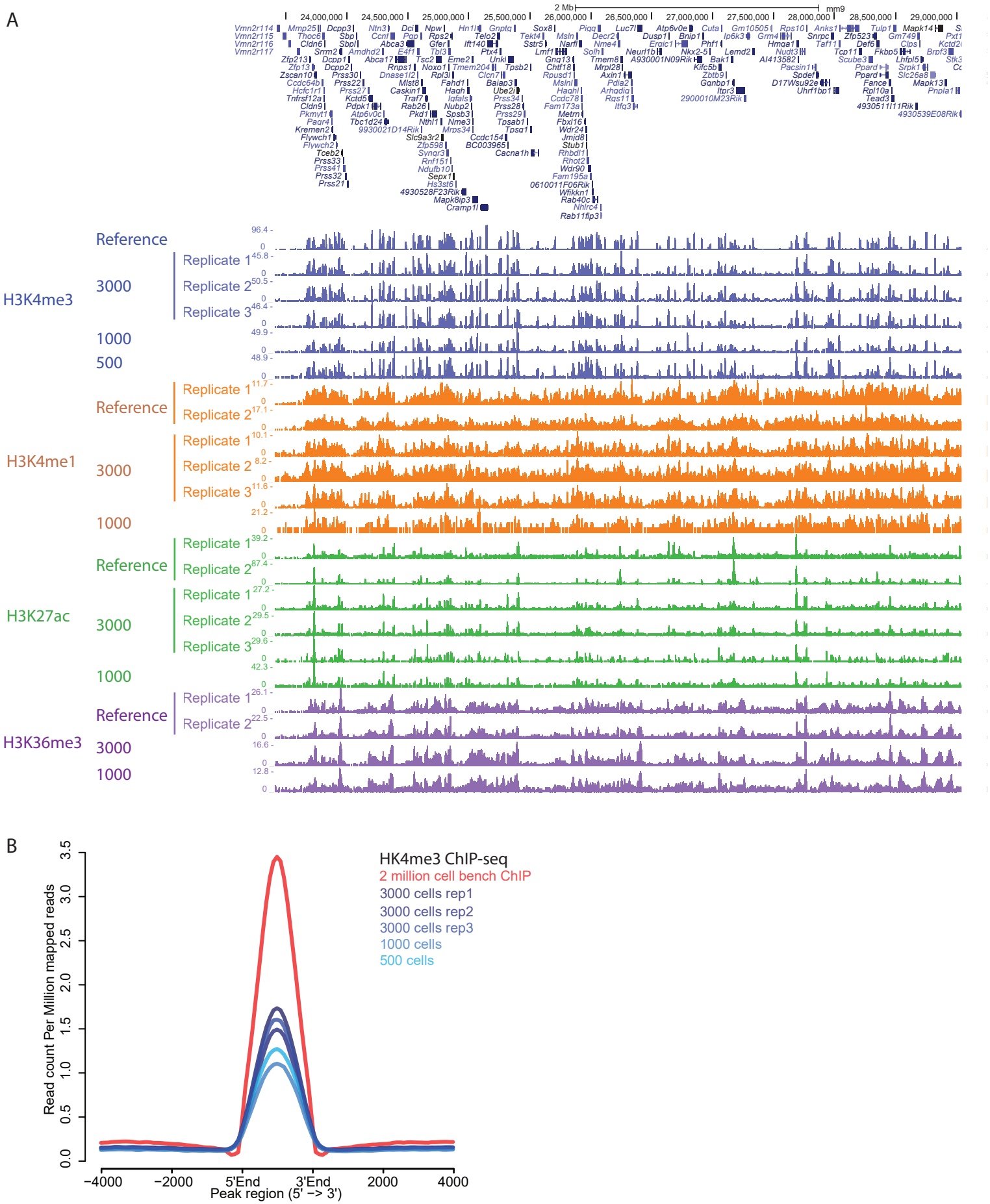

Supplemental Figure 6. PnP-ChIP-seq using small quantites of bulk-sonicated crosslinked chromatin. **(A)** Genome browser view of a 4Mb locus for PnP-ChIP-seq of H3K4me3, H3K4me1, H3K27ac and H3K36me3. **(B)** Average profile of H3K4me3 over all H3K4me3 peaks of profiles generated by PnP-ChIP-seq using small quantites of bulk-sonicated crosslinked chromatin. The start and end of the peaks are indicated with 5'end and 3'end, respectively.

Supplemental Figure 7

A

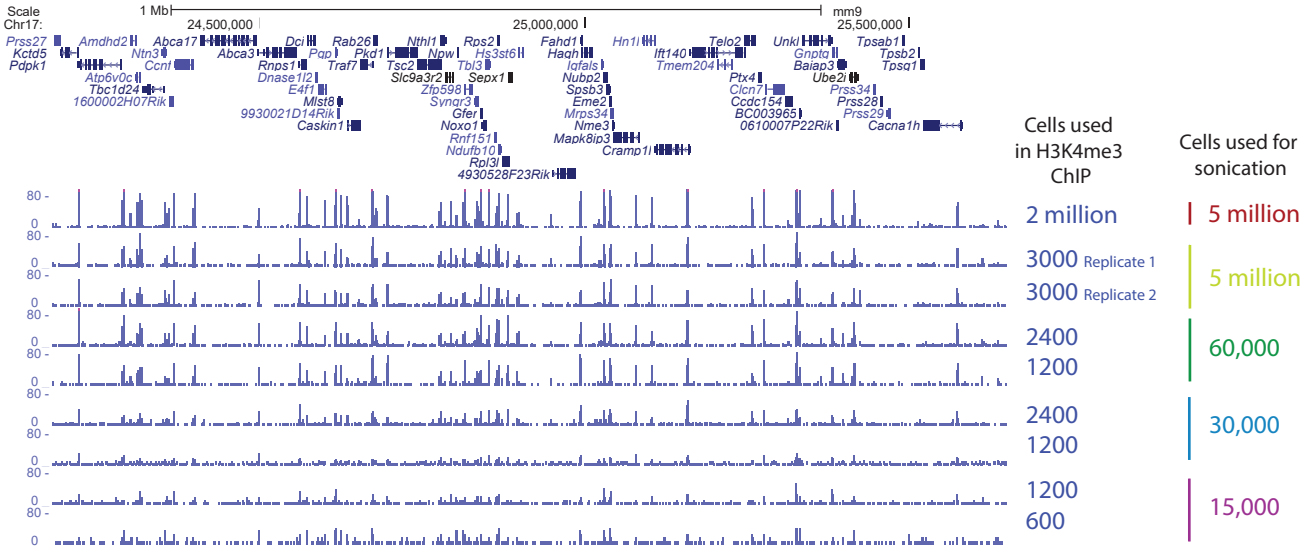

B

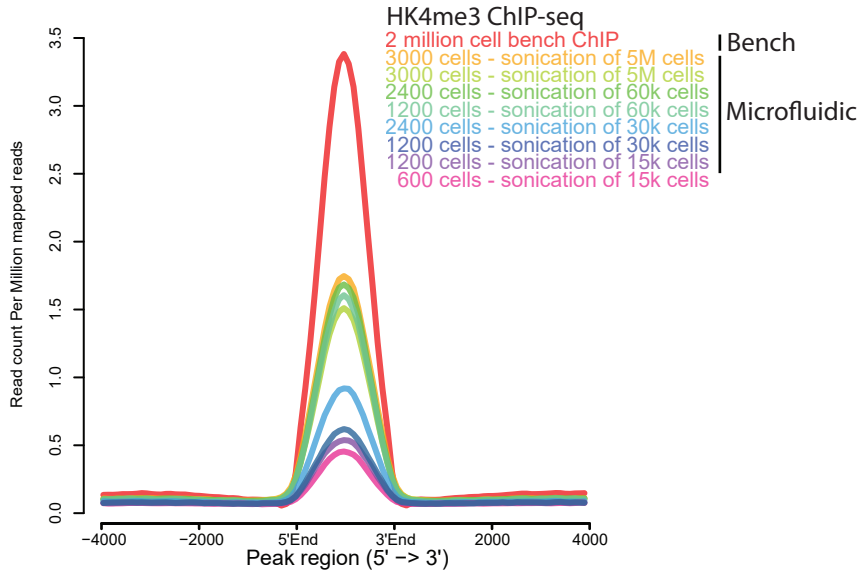

Supplemental Figure 7. Use of low-volume sonication on low numbers of mESCs for PnP-ChIP-seq. **(A)** Genome browser view of a gene-rich locus for PnP-ChIP-seq of H3K4me3 using a series of mESC input quantities for sonication. **(B)** Average profile of H3K4me3 over all H3K4me3 peaks of profiles generated by PnP-ChIP-seq using a series of mESC input quantities for sonication. The start and end of the peaks are indicated with 5'end and 3'end, respectively.

Supplemental Figure 8

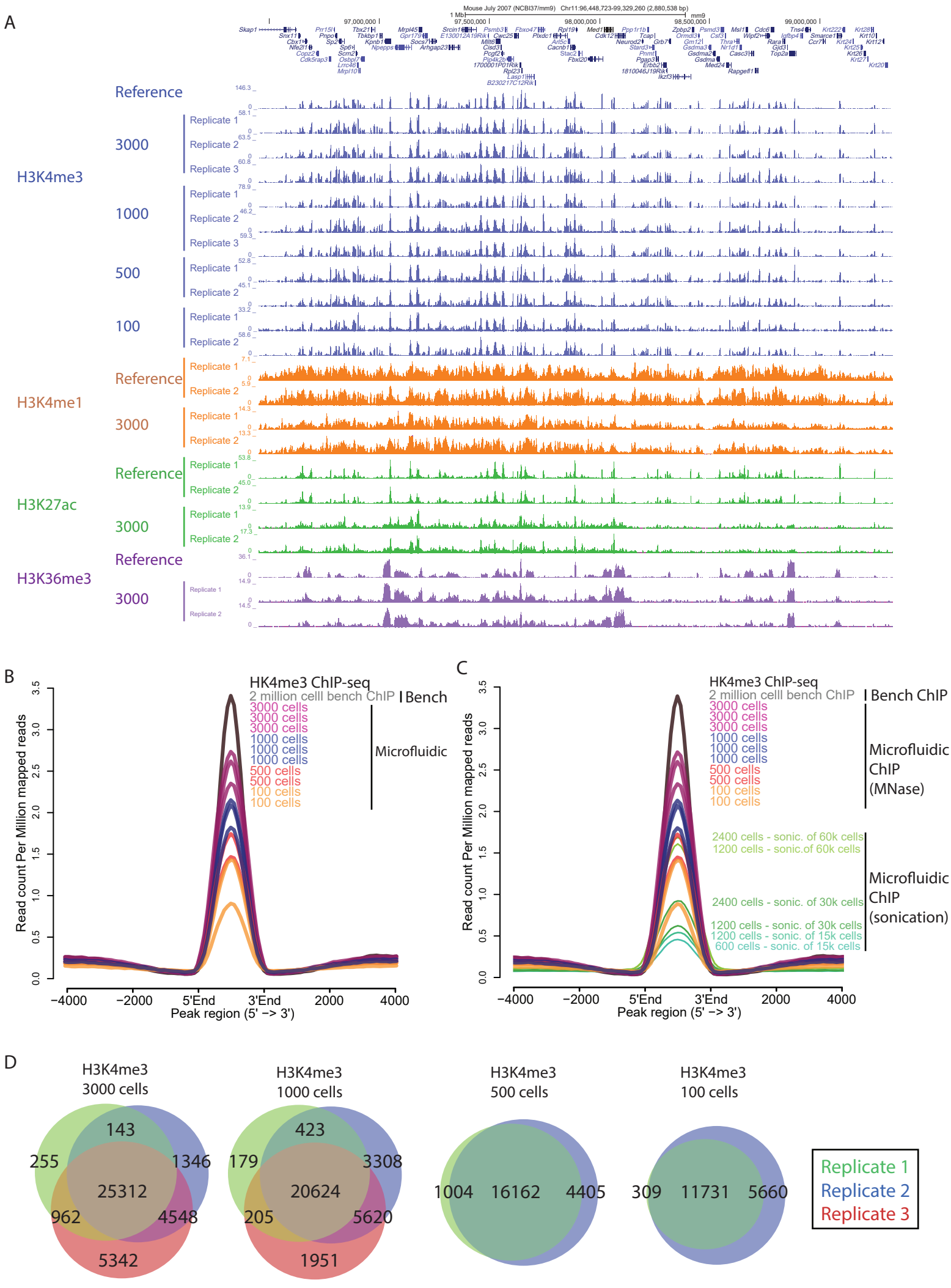

Supplemental Figure 8. PnP-ChIP-seq using small cell quantities by the use of MNase shearing on 15,000 mESCs. **(A)** Genome browser view of a 3Mb locus for PnP-ChIP-seq of H3K4me3, H3K4me1, H3K27ac and H3K36me3. **(B)** Average profile of H3K4me3 over all H3K4me3 peaks of profiles generated by PnP-ChIP-seq using small cell quantities by the use of MNase shearing on 15,000 mESCs. The start and end of the peaks are indicated with 5'end and 3'end, respectively. **(C)** A comparison of H3K4me3 over all H3K4me3 peaks of profiles generated by PnP-ChIP-seq using small cell quantities by the use of sonication or MNase shearing. The start and end of the peaks are indicated with 5'end and 3'end, respectively. **(D)** Overlap between de novo H3K4me3 peak calls of replicate PnP-ChIP-seq using small cell quantities by the use of MNase shearing on 15,000 mESCs.

Supplemental Figure 9

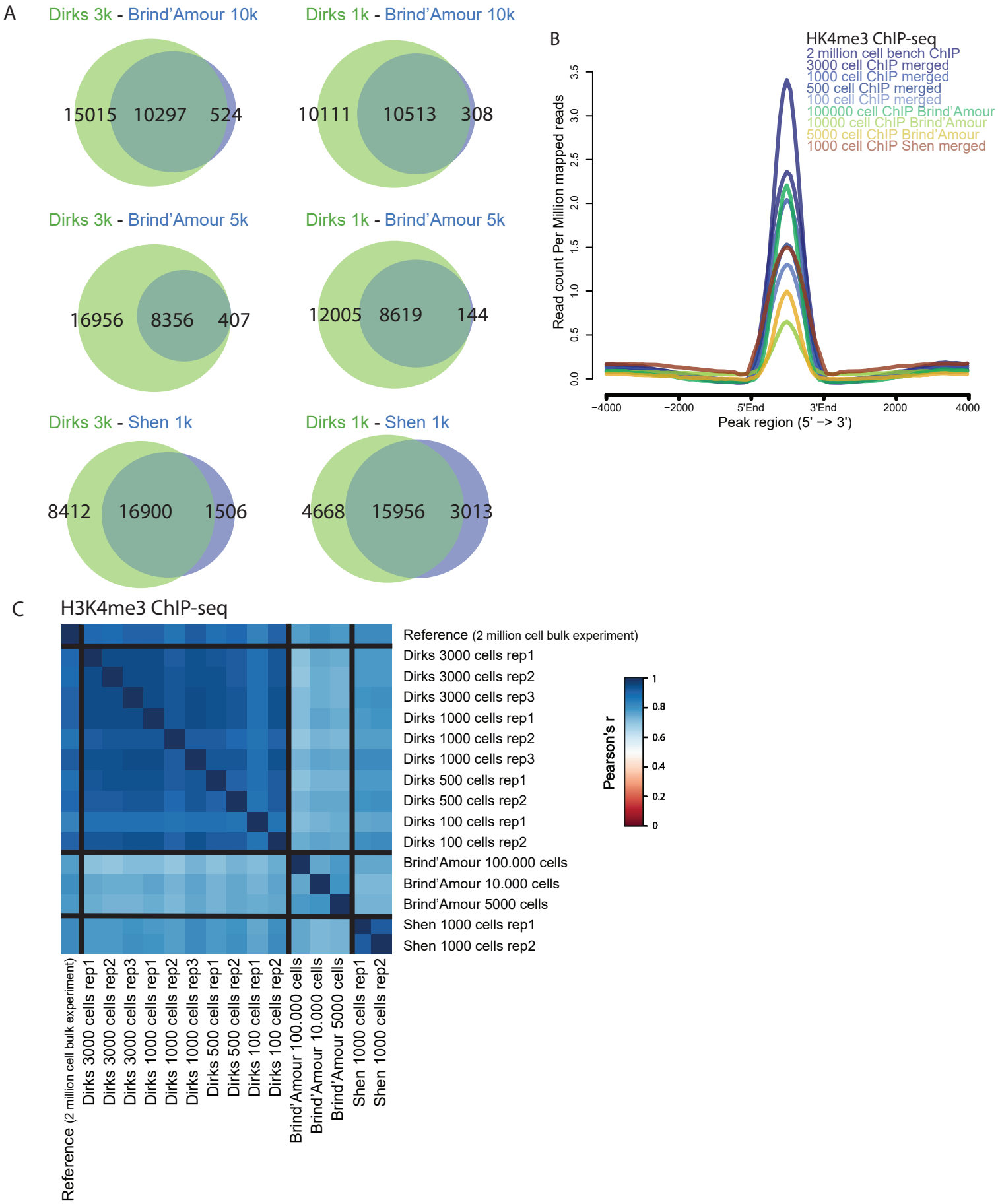

Supplemental Figure 9. Comparison between MNase-based PnP-ChIP-seq and alternative low-cell input ChIP-seq methods developed by (Brind'Amour et al., 2015) or an automated microfluidic platform developed by Shen et al. (2015) **(A)** Intersections between de novo peak calls of H3K4me3 PnP-ChIP-seq and H3K4me3 profiles generated using alternative low-cell input ChIP-seq. **(B)** Average profile of H3K4me3 over all H3K4me3 peaks of profiles generated by PnP-ChIP-seq using small cell quantities by the use of MNase shearing on 15,000 mESCs (in blue called "ChIP merged") or using H3K4me3 profiles generated by alternative low-cell input ChIP-seq methods performed on mESCs (in other colors). The start and end of the peaks are indicated with 5'end and 3'end, respectively. **(C)** Cross-correlation between H3K4me3 PnP-ChIP-seq (labeled "Dirks") and H3K4me3 profiles generated using alternative low-cell input methods for ChIP-seq.

Supplemental Figure 10

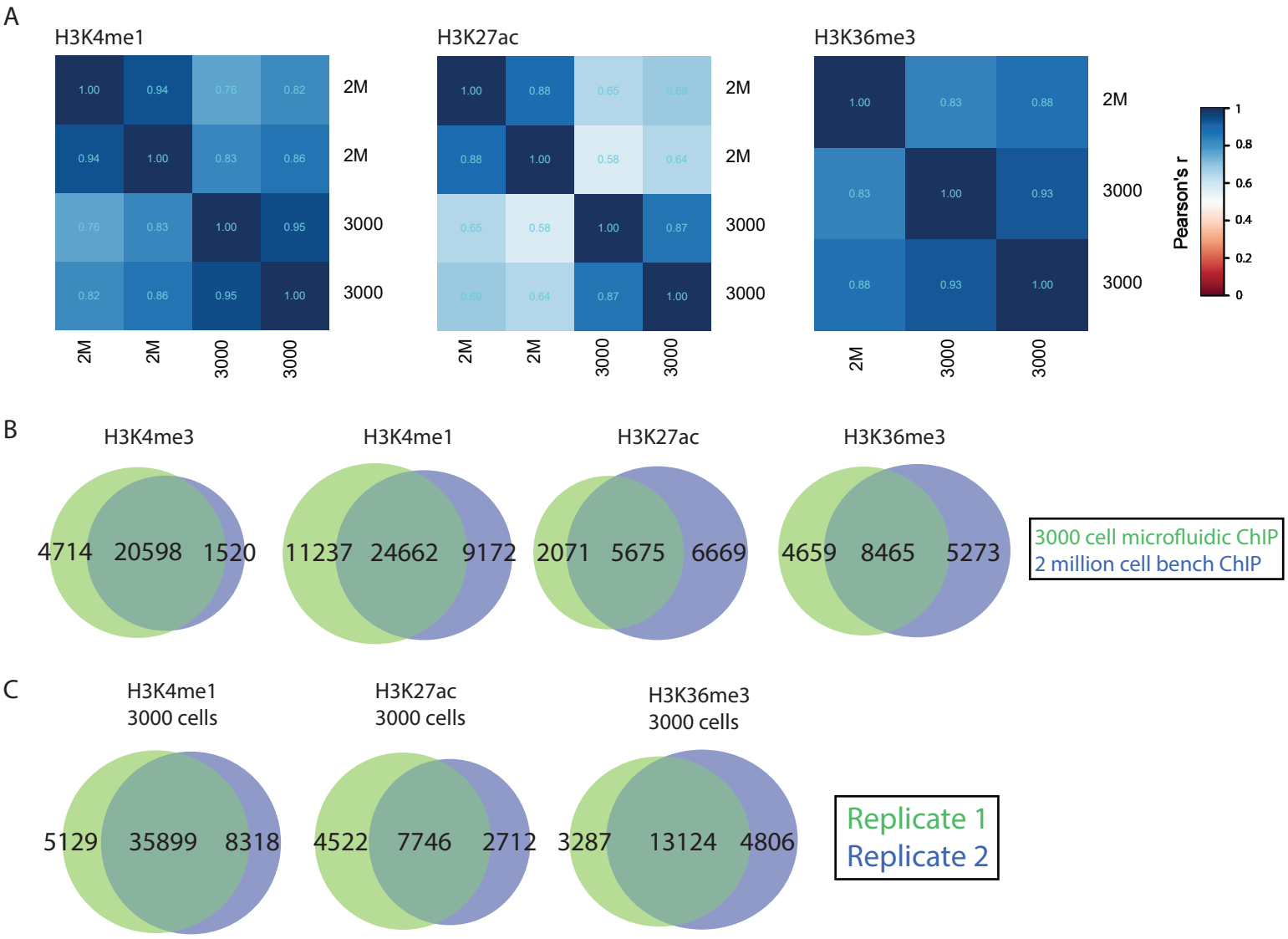

Supplemental Figure 10. PnP-ChIP-seq using small cell quantities using MNase shearing on 15,000 mESCs for H3K4me1, H3K27ac and H3K36me3. **(A)** Cross-correlations of PnP-ChIP-seq using tag counts of merged peak set for H3K4me1, H3K27ac or H3K36me3 **(B)** Overlap between de novo peak calls of PnP-ChIP-seq and bulk ChIP-seq. **(C)** Overlap between de novo peak calls of PnP-ChIP-seq of replicate experiments using 3000 mESC chromatin equivalent as input.

Supplemental Figure 11

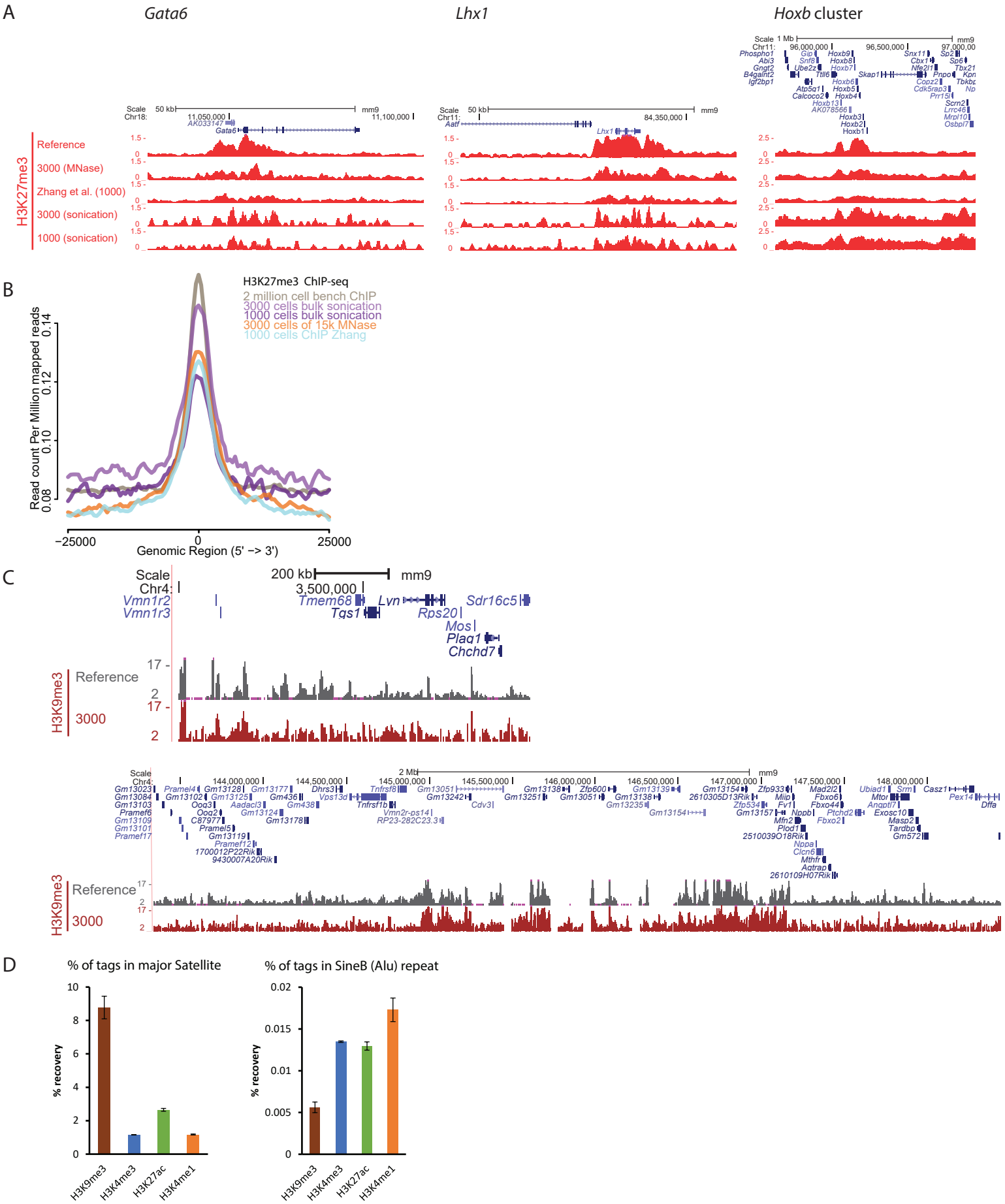

Supplemental Figure 11. PnP-ChIP-seq of H3K27me3 and H3K9me3. **(A)** Examplary genome browser views for PnP-ChIP-seq of H3K27me3. **(B)** Average profile of H3K27me3 over all H3K27me3 peaks in mESCs (van Mierlo et al., 2019) of profiles generated by PnP-ChIP-seq as compared to bulk ChIP-seq profiles and an alternative low-cell input ChIP-seq method called STAR ChIP-seq (Zhang et al., 2016). The start and end of the peaks are indicated with 5'end and 3'end, respectively. **(C)** Genome browser views for PnP-ChIP-seq of H3K9me3. The bottom example shows a genomic region which is highly enriched for major satellite repeats. **(D)** Presence of PnP-ChIP-seq sequence tags of various hPTMs in two types of repeats, confirming the presence of H3K9me3 over major satellites.

Supplemental Figure 12

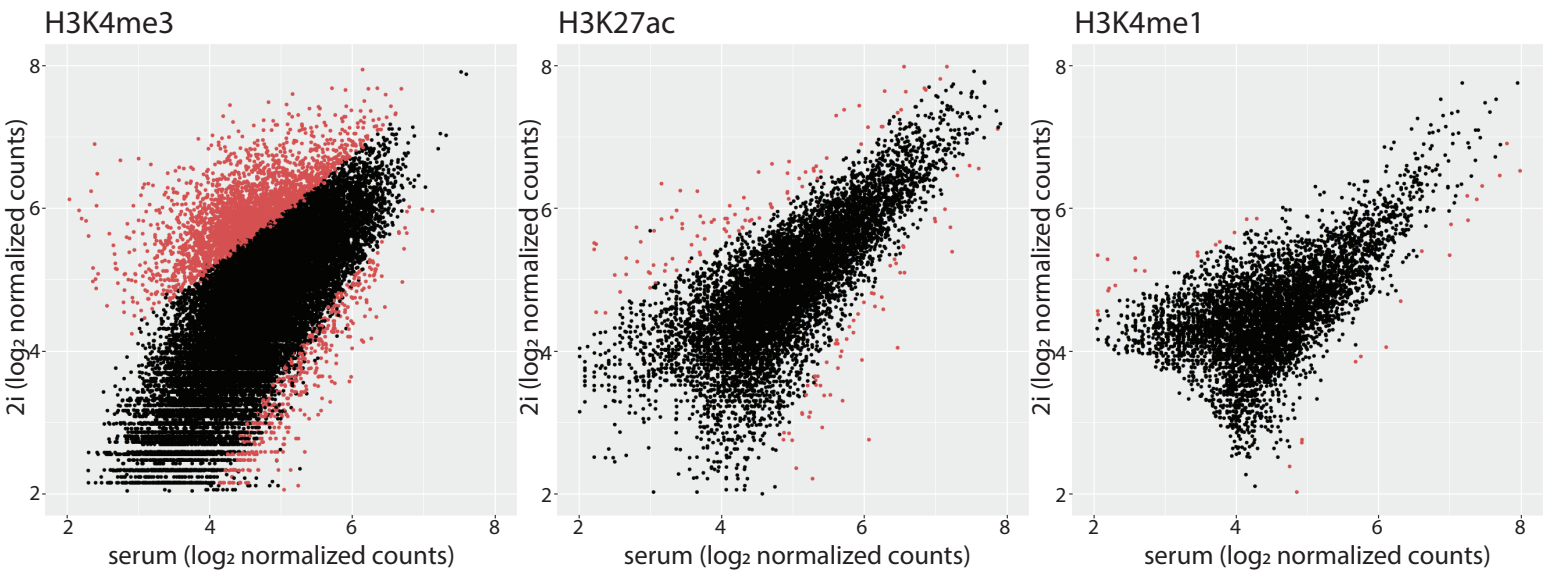

Supplemental Figure 12. PnP-ChIP-seq allows to detect significant differences in the closely-related cell types 2i and serum mESCs. Scatterplot of DESeq2-normalised tag counts (replicate means) of H3K4me3, H3K27ac and H3K4me1 PnP-ChIP-seq on 2i and serum mESCs. Significant enrichment (FDR-adjusted p-value < 0.05) depicted in red. We detect in total 25,617 H3K4me3 peaks (3,459 peaks significantly higher in either 2i ESCs or serum ESCs), 8,329 H3K27ac peaks (161 peaks significantly higher in either 2i ESCs or serum ESCs), and 5,752 H3K4me1 peaks (41 peaks significantly higher in either 2i mESCs or serum mESCs). Please find more details in Supplemental Table S1.

Supplemental Figure 13

A H3K4me3 ChIP-seq, significantly higher in 2i mESCs

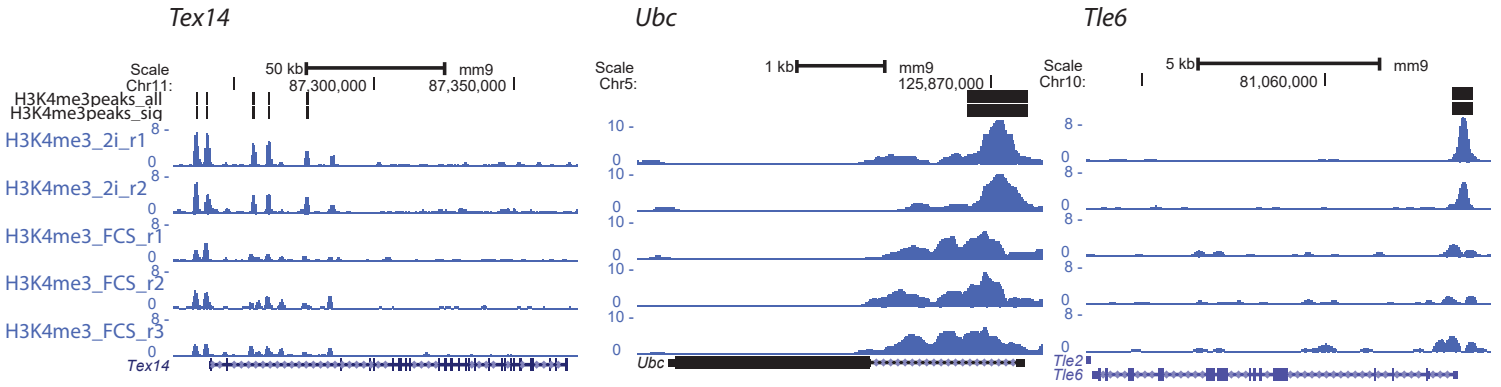

B H3K4me3 ChIP-seq, significantly higher in serum mESCs

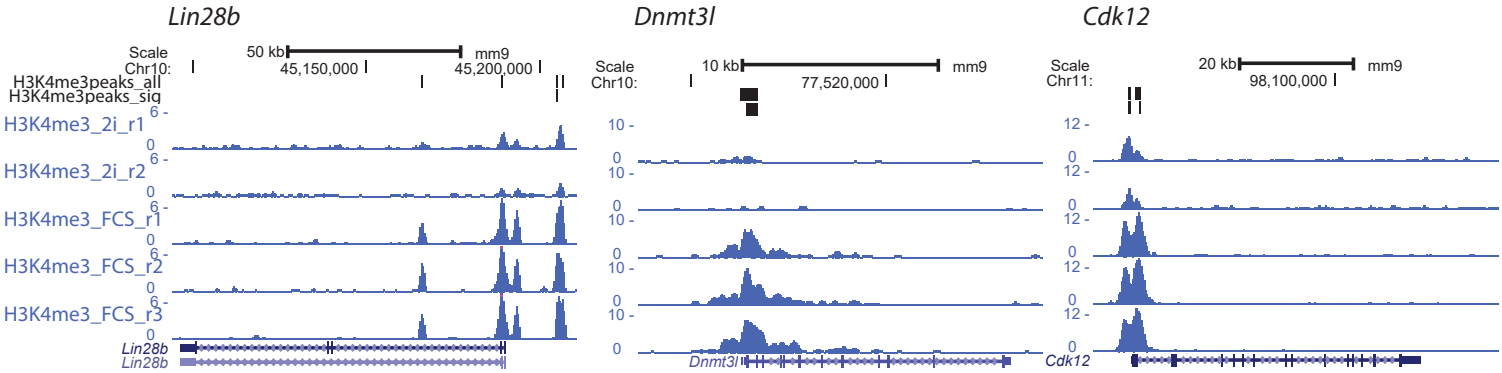

Supplemental Figure 13. PnP-ChIP-seq allows the detection of significant differences in H3K4me3 between the closely-related cell types 2i and serum ESCs (serum is abbreviated as FCS (foetal calf serum)). **(A)** Genome browser views for H3K4me3 PnP-ChIP-seq of 2i and serum mESCs for 3 genes that are known to be higher expressed in 2i mESCs. **(B)** Genome browser views for H3K4me3 PnP-ChIP-seq of 2i and serum mESCs for 3 genes that are known to be higher expressed in serum mESCs. r = replicate; H3K4me3peaks_all = merge track of all H3K4me3 peaks detected in 2i mESCs and serum mESCs. H3K4me3peaks_sig = merge track of all H3K4me3 peaks that are significantly increased in either 2i mESCs or serum mESCs. Significant differences in gene expression between 2i and serum ESCs from Marks et al., 2012 (PMID: 22541430).

Supplemental Figure 14

A H3K27ac ChIP-seq, significantly higher in 2i mESCs

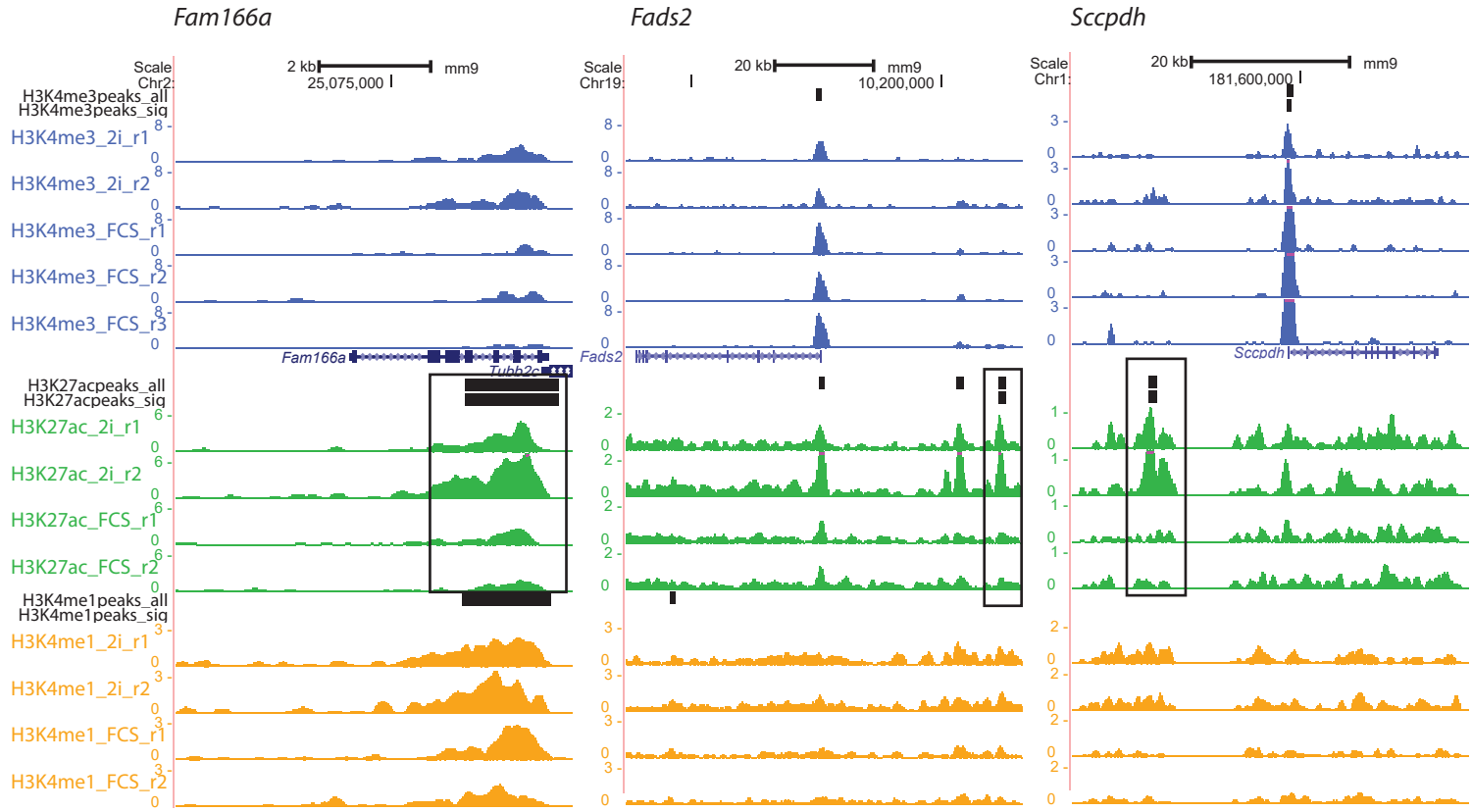

B H3K27ac ChIP-seq, significantly higher in serum mESCs

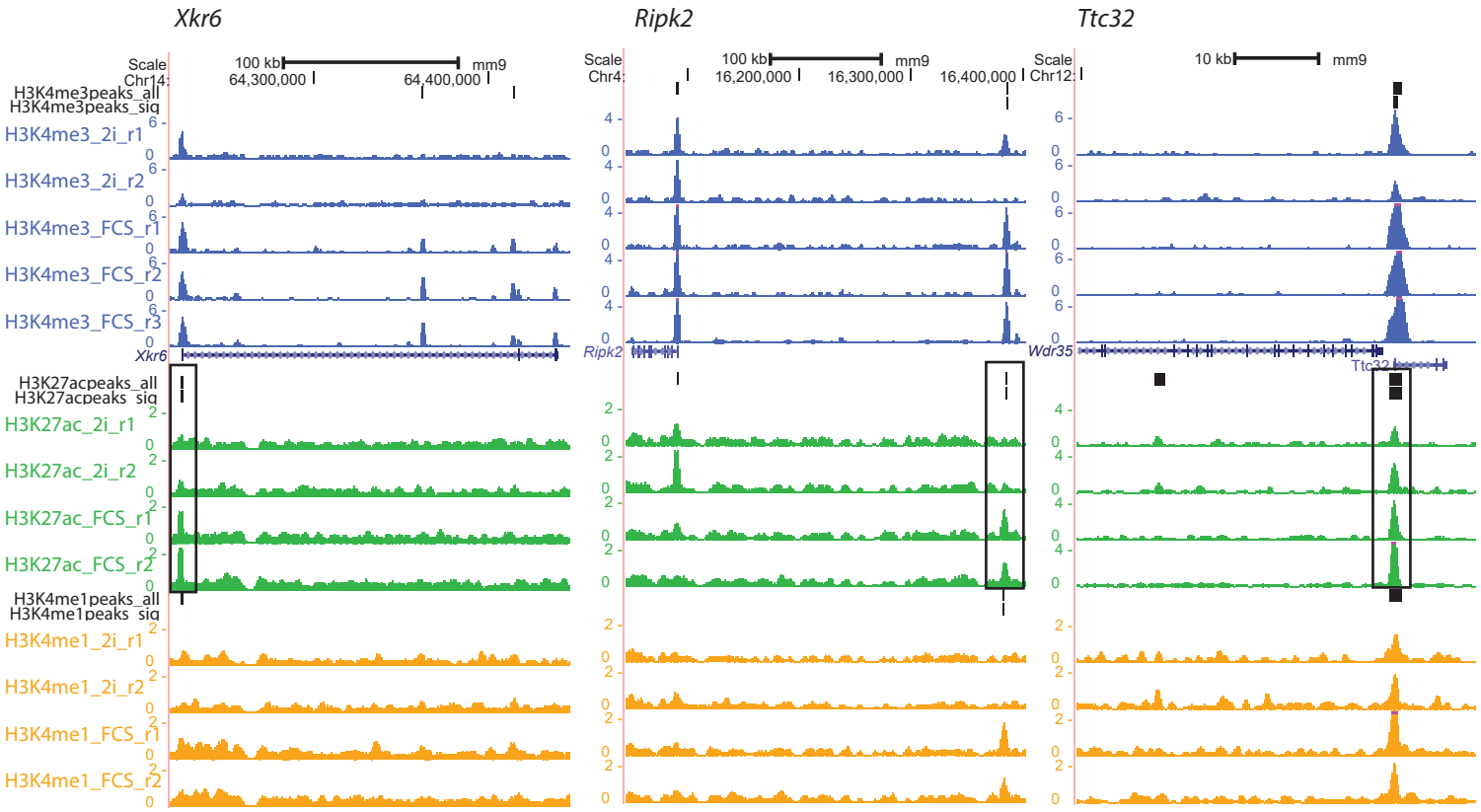

Supplemental Figure 14. PnP-ChIP-seq allows the detection of significant differences in H3K27ac between the closely-related cell types 2i and serum ESCs (serum is abbreviated as FCS (foetal calf serum)). **(A)** Genome browser views for PnP-ChIP-seq of loci showing a significant increase in H3K27ac in 2i mESCs as compared to serum mESCs (boxed) **(B)** Genome browser views for PnP-ChIP-seq of loci showing a significant increase in H3K27ac in serum mESCs as compared to 2i mESCs (boxed). r = replicate; H3*peaks_all = merge track of all peaks of a hPTM detected in 2i mESCs and serum mESCs. H3*peaks_sig = merge track of all peaks of a hPTM that are significantly increased in either 2i mESCs or serum mESCs.

Supplemental Figure 15

A H3K4me1 ChIP-seq, significantly higher in 2i mESCs

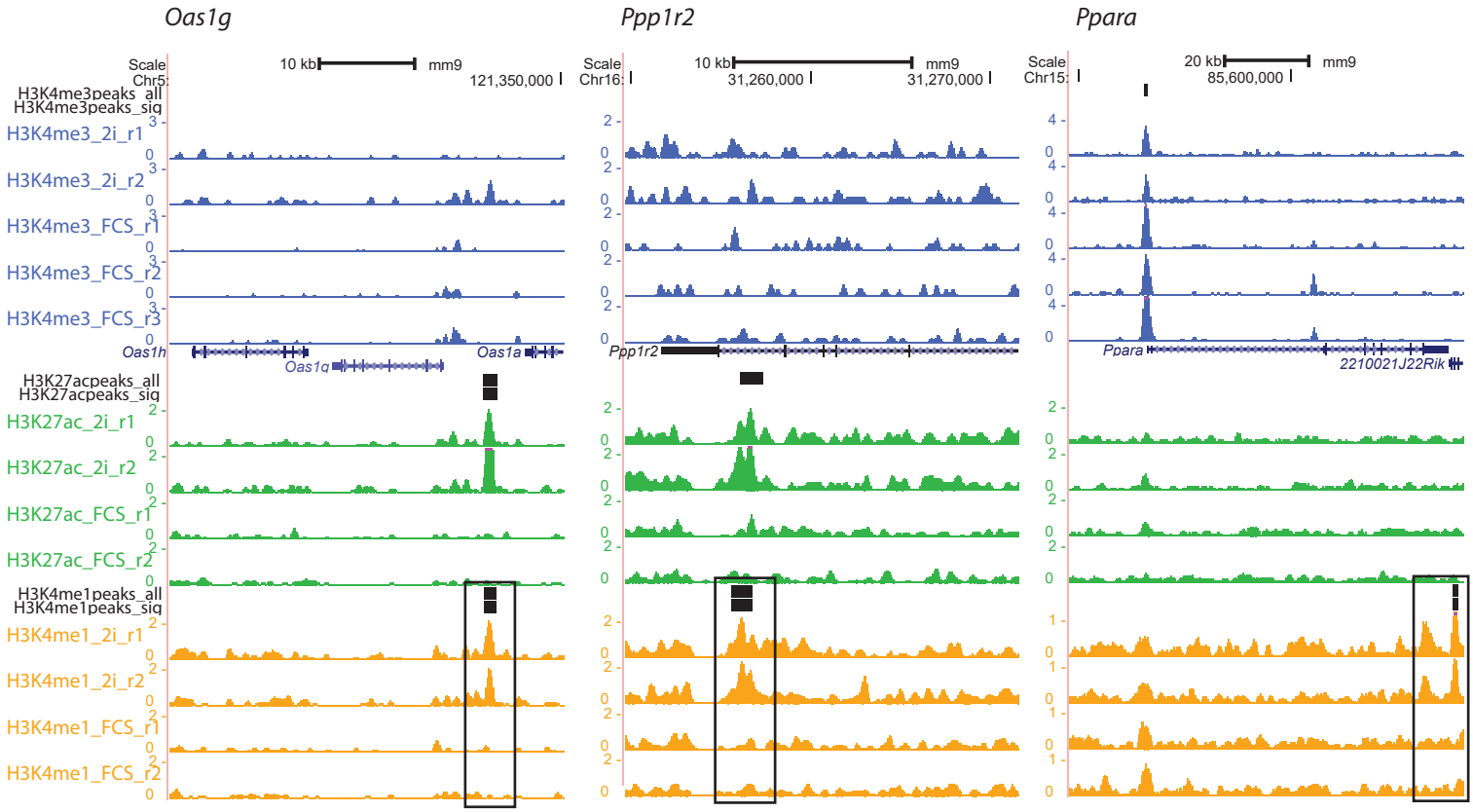

B H3K4me1 ChIP-seq, significantly higher in serum mESCs

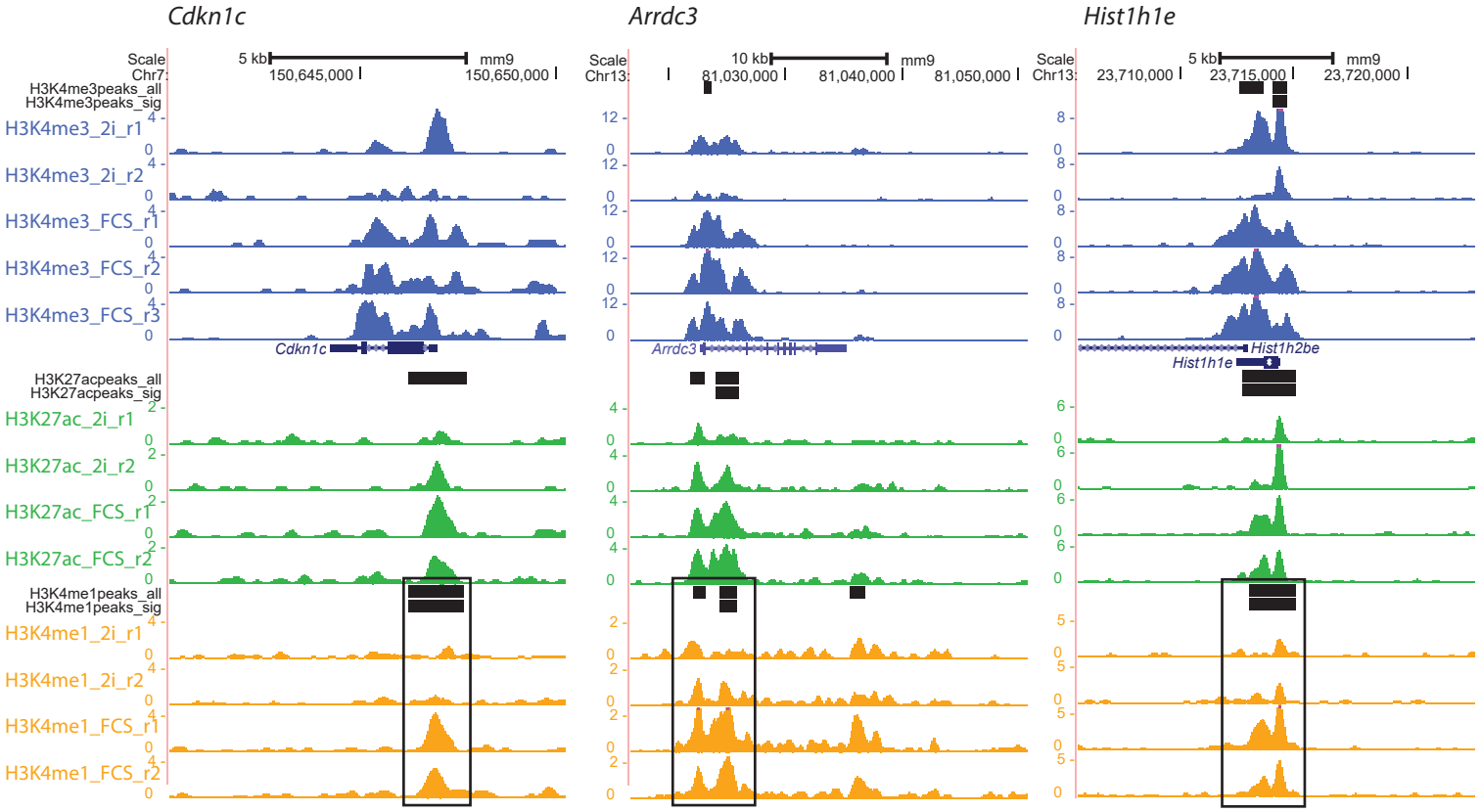

Supplemental Figure 15. PnP-ChIP-seq allows the detection of significant differences in H3K4me1 between the closely-related cell types 2i and serum ESCs (serum is abbreviated as FCS (foetal calf serum)). **(A)** Genome browser views for PnP-ChIP-seq of loci showing a significant increase in H3K4me1 in 2i mESCs as compared to serum mESCs (boxed) **(B)** Genome browser views for PnP-ChIP-seq of loci showing a significant increase in H3K4me1 in serum mESCs as compared to 2i mESCs (boxed). r = replicate; H3*peaks_all = merge track of all peaks of a hPTM detected in 2i mESCs and serum mESCs. H3*peaks_sig = merge track of all peaks of a hPTM that are significantly increased in either 2i mESCs or serum mESCs.

Supplemental Figure 16

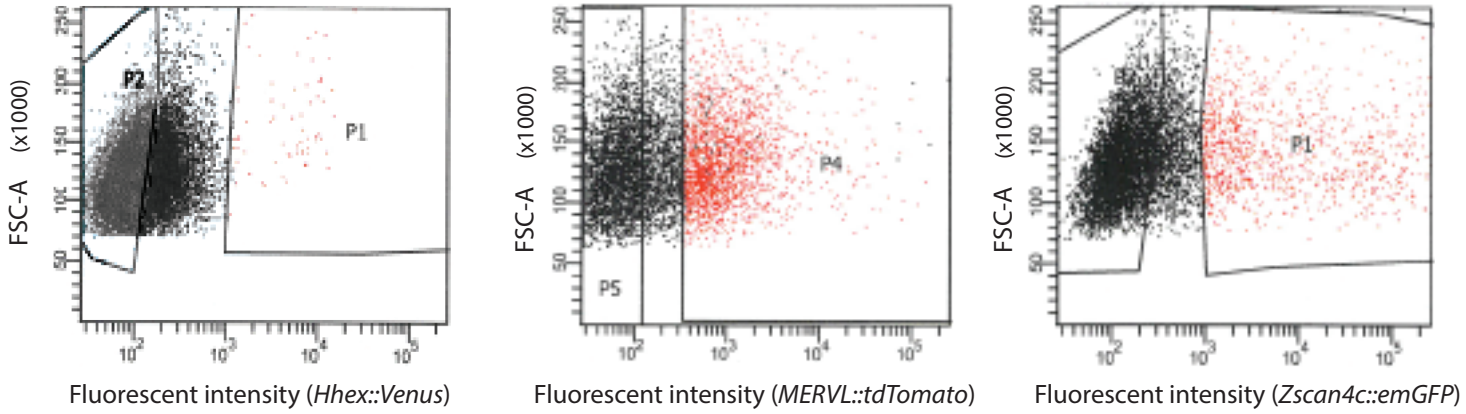

Supplemental Figure 16. Gating of embryonic stem cell subpopulations on fluorescent markers Venus (driven by the *Hhex* promoter), tdTomato (driven by the MERVL promoter) and emGFP (driven by the *Zscan4c* promoter).

Supplemental Figure 17

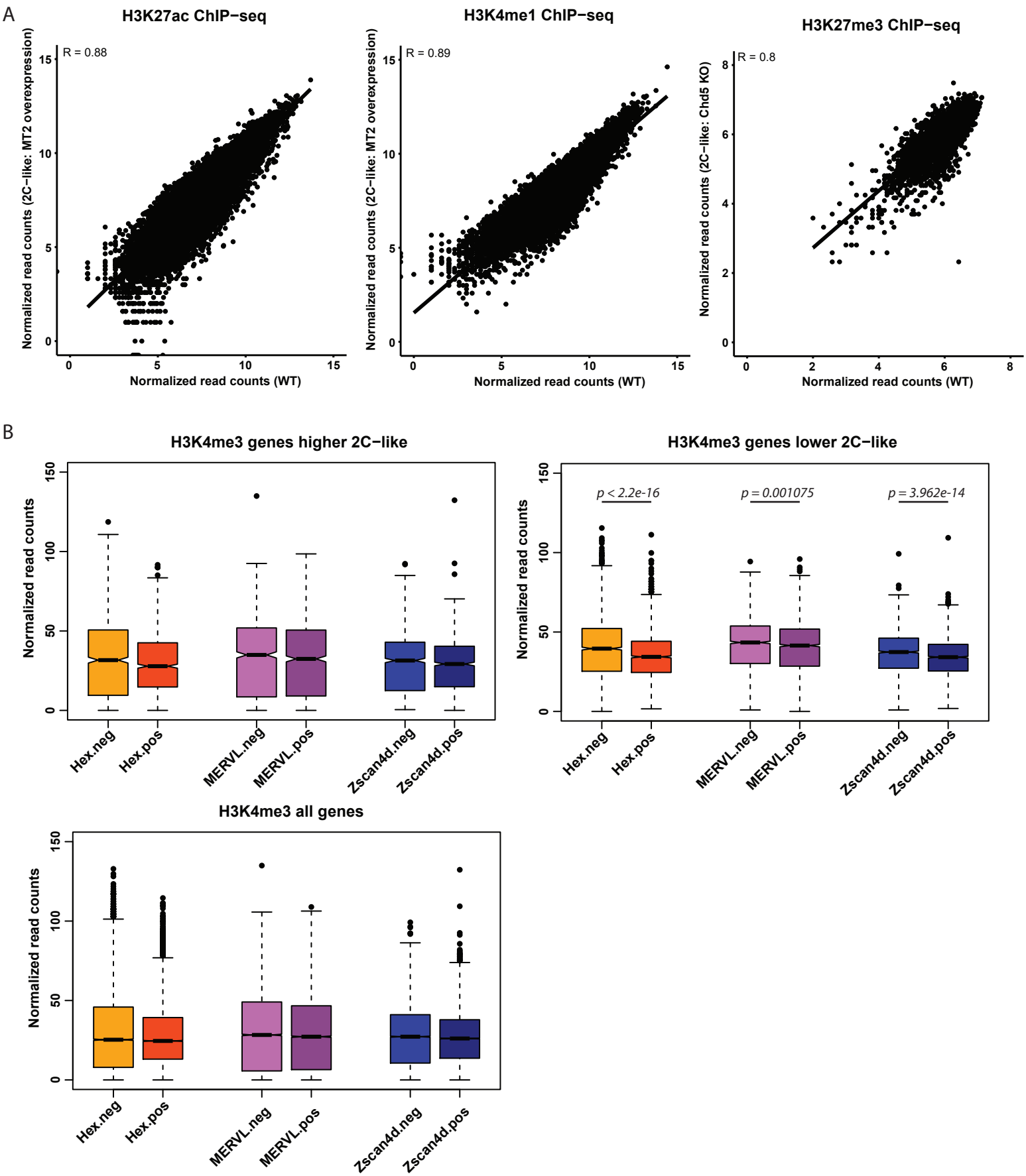

Supplemental Figure 17. Epigenome analysis of 2C-like cells as compared to wildtype mESCs. **(A)** Scatterplot of DESeq2-normalised ChIP-seq tag counts of H3K27ac, H3K4me1 (both from Zhang et al., 2019) and H3K27me3 (Hayashi et al., 2016) of 2C-like cells as compared to wildtype mESCs. DESeq2 analysis detected no significant differences (FDR-adjusted p-value < 0.05) in H3K27ac, H3K4me1 or H3K27me3 between 2C-like cells and wildtype mESCs. The axes of the plots are in $\log_2$. **(B)** Boxplots of DESeq2-normalised tag counts of H3K4me3 PnP-ChIP-seq profiles of Hhex-, MERVL- and Zscan4c-positive ("pos") and negative ("neg") mESC cell populations of all genes, and genes that have been reported to be higher of lower in 2C-like cells as compared to wildtype mESCs (Fu et al., 2019). Significant differences between boxplots calculated using the Wilcoxon rank-sum test are indicated.